

# Ring-Like Structure in the Radio Lobe of MG0248+0641

*Submitted to AJ: August 15, 1997; Accepted: September 30, 1997*

Samuel R. Conner<sup>1</sup>, Asantha R. Cooray<sup>1,2</sup>, André B. Fletcher<sup>1</sup>, Bernard F. Burke<sup>1</sup>, Joseph Lehar<sup>3</sup>, Peter M. Garnavich<sup>3,4</sup>, Tom W. B. Muxlow<sup>5</sup>, Peter Thomasson<sup>5</sup>, John P. Blakeslee<sup>6</sup>

## ABSTRACT

We present radio and optical observations of MG0248+0641, which contains a kiloparsec-scale ring-like structure in one of its radio lobes. The radio observations show a typical core-double morphology: a central core between two lobes, each of which has a hotspot. The western radio lobe appears as a nearly continuous ring, with linear polarization electric field vectors which are oriented in a radial direction from the ring center. We consider several different interpretations for the nature of this ring, including gravitational lensing of a normal jet by a foreground galaxy. Even though simple lensing models can describe the ring morphology reasonably well, the high linear polarization seen around the ring cannot be easily explained, and no lensing object has yet been found in deep optical and infrared searches within the extent of the ring. If the radio ring is indeed caused by gravitational lensing, the implied mass-to-light ratio is typical of the very high values seen in other candidate “dark” gravitational lenses. The chance interposition of a galactic supernova remnant, nova, planetary nebula, or H II region, has been ruled out. The highly polarized ring of MG0248+0641 is much like the prominent ring seen in 3C219, and the multiple ones in 3C310 and Hercules A, suggesting that similar physical processes are producing shell structures in these radio galaxies. The ring in MG0248+0641 may be caused by the formation of “bubbles”, as a result of instabilities in the energy flow down the western radio jet. It may also be possible that the required instabilities are triggered by the infall of gas, via tidal interaction of the central source with a nearby galaxy. This scenario may be indicated by our marginal detection of an optical source close to the western hotspot.

---

<sup>1</sup>Department of Physics, Massachusetts Institute of Technology, 77 Massachusetts Avenue, Cambridge MA 02139, USA.

<sup>2</sup>Now at Department of Astronomy and Astrophysics, University of Chicago, Chicago IL 60637, USA. E-mail: asante@hyde.uchicago.edu.

<sup>3</sup>Center for Astrophysics, 60 Garden Street, Cambridge MA 02138, USA.

<sup>4</sup>Visiting Astronomer, Kitt Peak National Observatory, National Optical Astronomical Observatories, which is operated by the Association of Universities for Research in Astronomy (AURA) under cooperative agreement with the National Science Foundation.

<sup>5</sup>Nuffield Radio Astronomy Laboratories, Jodrell Bank, Cheshire SK11 9DL, UK.

<sup>6</sup>Palomar Observatory, California Institute of Technology, MS 105-24, Pasadena CA 91125, USA.

*Subject headings:* radio galaxies: individual (MG0248+0641) — active galactic nuclei  
- radio jets and lobes.

## 1. Introduction

The MIT-Green Bank-VLA (MG-VLA) lens search surveys (Lawrence *et al.* 1986; Hewitt 1986; Lehár 1991; Herold-Jacobson 1996) have so far produced six confirmed lenses from snapshot maps of about 6000 sources: MG0414+0534 (Hewitt *et al.* 1992), MG0751+2716 (Lehár *et al.* 1997), MG1131+0456 (Hewitt *et al.* 1988), MG1549+3047 (Lehár *et al.* 1993), MG1654+1346 (Langston *et al.* 1989), and MG2016+112 (Lawrence *et al.* 1984). After an extensive improvement in mapping procedures the same data in the MG-VLA survey have been reanalyzed, the result being a promising subsample of radio sources with morphologies typical of gravitational lensing (Conner *et al.* 1993). Included in this was MG0248+0641, which, after recalibration and remapping of the original 6 cm data, showed an unusual ring-like structure in the total intensity map.

At 6 cm (4.85 GHz), the source has a measured single-dish flux density of  $300 \pm 38$  mJy (Becker *et al.* 1991), and at 20 cm (1.4 GHz)  $804 \pm 60$  mJy (White & Becker 1992), indicating an integrated spectral index  $\alpha \sim -0.8$  ( $S_\nu \sim \nu^\alpha$ ), which is moderately steep. The radio structure in MG0248+0641 (probably 4C+06.13) was first mapped by Lawrence *et al.* (1986) as part of a program to discover gravitational lenses in the MIT-Green Bank (MG) catalog. The observations were made with the NRAO <sup>7</sup> Very Large Array (VLA) A-array configuration for an on-source integration time of  $\sim 2$  minutes. Although the resolution was  $\sim 0''.3$ , the original calibration and mapping of the data were not good enough to uncover the detailed structure of the extended emission.

As rings are a rare type of morphology within the MG-VLA sample, MG0248+0641 has now been observed with the VLA at 2 cm (14.9 GHz), 3.6 cm (8.4 GHz) and 6 cm (4.6 GHz), and with MERLIN at 18 cm (1.6 GHz). Optical and infrared observations of the field containing the source have been made in R-band with the 2.4 m Hiltner telescope of the Michigan-Dartmouth-MIT (MDM) Observatory and in K-band with the KPNO 2.1 m telescope, respectively. The MDM 2.4 m and MMT have been used to obtain spectra of optical sources within one arcminute of MG0248+0641. These observations were carried out initially to determine the lensing nature of this radio source.

---

<sup>7</sup>The National Radio Astronomy Observatory (NRAO) is a facility of the National Science Foundation operated under cooperative agreement by Associated Universities, Inc.

## 2. Observations

New VLA observations of MG0248+0641 have been made in the A-array at 3.6 and 6 cm in August 1995, and in B-array at 2 cm in October 1995. The on-source integration times of the 2, 3.6 and 6 cm observations were 40, 20, and 20 minutes respectively. Calibration and mapping of these data were performed using standard AIPS procedures. The maps were further self-calibrated, yielding final rms noise levels of typically twice the thermal limit.

The 1995 VLA maps are shown in Fig. 1. The overall structure of the source is a double-sided core-jet-hotspot system. The 3 bright peaks correspond to the central core and two hotspots, with the core being located at  $\alpha=02:48:58.28$ ,  $\delta=06:41:43.6$  (J2000), with an astrometric accuracy of  $\sim 0''.2$  (Lawrence *et al.* 1986). In the 3.6 cm map, the integrated flux densities of the core, western and eastern hotspots are 9, 23 and 3.2 mJy, respectively. The noise level in this map is  $\sim 0.1$  mJy beam $^{-1}$ . The western lobe contains a prominent ring-like structure in between the core and western hotspot, and there appears to be a large extended area of diffuse emission north of this ring, which is most distinctively imaged in the 3.6 cm map. Diffuse low surface-brightness emission envelopes the ring and the eastern jet, though this is not well imaged by the CLEAN deconvolution algorithm. We do find several knots within this diffuse emission, on both sides of the core. At the sensitivity of our observations, there is no evidence for an undisturbed jet to the west of the core, but we detect a partial jet east of the core. In Fig. 2 we show the spectral index distribution of MG0248+0641, based on the VLA 2 and 6 cm observations, where the 6 cm A-array emission has been convolved to the 2 cm B-array resolution. The ring-like structure has a spectral index of  $\sim -1.0$ , whereas the core component is found with a spectral index of  $\sim -0.6$ . The two hotspots are found with a varying spectral index distribution, with an index value close to  $\sim -0.5$  at the ends closest to the core, and highly steep values  $\sim -1.5$  at the post-shock endpoints. All of these values are consistent with the integrated index  $\alpha \sim -0.8$  from the single-dish measurements.

VLA linear polarization maps were made from all of the 1995 data, at each of the observed wavelengths, using observations of 3C48 as a polarization calibrator based on the polarization angle values given in Perley (1982). In Fig. 3, we show the total intensity contour plots of the radio emission, onto which we have overlaid the fractional linear polarization electric field E vectors. The ring exhibits high fractional linear polarization, from 20% to 70%, with vectors oriented radially outward from the ring center. The orientations of these vectors do not change by more than  $\sim 10$  degrees between 2 and 6 cm, indicating a small Faraday rotation in this wavelength range. Therefore, these vectors should be perpendicular to the magnetic flux density B field lines in the emitting plasma of the radio galaxy, assuming that the radiation is primarily due to the synchrotron process. The hotspots are 12% polarized. The diffuse emission north of the ring has a fractional polarization of only  $\sim 5\%$ , and it is noted that this falls to an unmeasurable value in the central and brightest part of this emission. The partial jet to the east of the core is 15% polarized. Thus, emission from non-ring portions of this source are weakly polarized ( $\leq 15\%$ ), while the ring and its associated structures are highly polarized. In the brighter, outermost part of the eastern jet, the polarization vectors are oriented along the axis of the jet, but rotate towards the transverse

direction as the jet arrives at the hotspot.

We also observed MG0248+0641 with the MERLIN array in May 1997, using 7 antennae at 18 cm, with an on-source integration time of  $\sim 8$  hours. The observations of the source were phase referenced to the compact calibration source 0246+061 (Browne *et al.* 1997). 3C286, together with 0246+061, were used as polarization calibrators, assuming a polarization position angle of 33 degrees for 3C286 at 18 cm. The data were edited, calibrated and mapped using standard MERLIN-D programs and procedures within AIPS. The resulting map (Fig. 4) has a resolution of  $0''.25$ . In Fig. 4, the core, western and eastern hotspot components are labeled A, B and C, with integrated flux densities of 14, 141, and 27 mJy, respectively. Several resolved knots of emission in and around the ring are seen. The partial eastern jet is also resolved into several knots, and the gap remains between the core and this jet, at this frequency. In Fig. 5, we show the MERLIN 18 cm fractional polarization map, with vectors overlaid onto the contour map of the total intensity. At this wavelength, it can be seen that the orientations of the vectors have changed by more than 70 degrees, especially along the arc-like feature adjacent to the western hotspot, suggesting a high Faraday rotation at this longer wavelength.

Based on astrometry using the Cambridge Automated Plate Measuring machine (APM) catalog, we found a faint optical counterpart at  $\alpha=02:48:58.23$ ,  $\delta=06:41:43.3$  (J2000). This source is  $0''.6$  southwest of the radio core, but does not lie inside the ring. Bearing in mind an estimated accuracy of 1 arcsecond in the APM position, we consider this source to be the optical counterpart of the radio core, and its position is marked with a cross in Fig. 4.

Optical observations of this field were carried out in visible wavelengths at the MDM 2.4 m Hiltner telescope in November 1995, and in the infrared K-band using the InSb  $256 \times 256$  array on the KPNO 2.1 m telescope in January 1996, with total integration times of 50 and 54 minutes, respectively. The data were reduced using standard procedures in IRAF. In Fig. 6 we show a  $4.5'$  by  $4.5'$  field from the 2.4 m telescope, imaged to a limiting magnitude of  $R \sim 25.5$ , with a seeing of  $0.89''$  (FWHM). The photometric observations of the object considered to be the optical counterpart of the radio core (marked by a square box in Fig. 6 and henceforth referred to as the counterpart) indicate an R magnitude of  $\sim 18.6$ , and color R-K of  $\sim 2.8$ . This counterpart is marginally resolved, with a circular isophote of  $\sim 0''.92$ , and subtracting a stellar point-spread-function revealed a possible host galaxy underneath. There are two other nearby sources to the west of the core counterpart (see Fig. 7). The first is  $3''.8$  away at  $\alpha = 02:48:57.98$ ,  $\delta = 06:41:42.9$  (J2000) with  $R \sim 24.7$  ( $2.1 \sigma$ ). The second is  $9''$  away at  $\alpha = 02:48:57.62$ ,  $\delta = 06:41:44.3$  (J2000), with  $R \sim 22.6$  ( $5.9 \sigma$ ) and  $K \sim 17.3$  ( $9 \sigma$ ), and which is slightly extended with  $\sim 1''.06$  (FWHM). The first source is probably detected in the infrared image with  $K \sim 18.8$  ( $3.2 \sigma$ ). However, the positions of the peaks of this very faint optical and infrared source do not match precisely; this is understandable as being due to the low signal-to-noise level in both R and K detections, and also due to known problems with the KPNO 2.1 m tracking in the infrared image.

Amongst the several objects within 1 arcminute of the counterpart, there are two galaxies

to the south, and two stars, one to the north and one to the east of it. The star to the east is obviously a foreground star in our own galaxy, and therefore has not been observed further. However, moderate resolution spectra have been obtained in November 1995 for the three other objects using the MODSPEC spectrograph on the MDM 2.4 m telescope. The star to the north is a late type star, with strong Fe I and Fe II lines, and a thermal spectrum of  $T \sim 5000$  K. Based on  $H\beta$  and [O III] 4959 and 5007 Å emission lines, the two galaxies to the south, with R magnitudes of  $\sim 15.7$  and 16.1, have been shown to be at the same redshift of 0.1.

In December 1995, we used the Blue Channel spectrograph on the MMT to obtain a 45 minute spectrum of the core counterpart. Two 1200s exposures were combined to produce the final spectrum in Fig. 8. The 300 grooves  $\text{mm}^{-1}$  grating and 1" slit provided a spectral resolution of  $\sim 5\text{\AA}$  (FWHM). The standard star BD28+4211 was used for flux calibration. The spectrum was extracted and calibrated using standard routines in IRAF. The spectrum has an unusually blue continuum ( $F_\nu \sim \nu^\alpha$ ,  $\alpha \sim 4.1$ ), which drops rapidly shortward of 6280 Å, corresponding to 4000 Å in the rest-frame, and levels off sharply to a flat continuum at longer wavelengths. The spectrum shows a broad Mg II 2798 Å emission line at 4408 Å, and two narrow [O III] 4959 Å and 5007 Å emission lines, at 7786 Å and 7881 Å, respectively. These lines suggest a redshift of 0.57 for the radio core. The absorption features in the spectrum, other than prominent atmospheric lines, have equivalent widths no greater than  $\sim 6$  Å, and may result from stars in the host galaxy of the AGN core counterpart, rather than from intervening absorbers. We have also detected the 3000 Å bump, commonly known as the “weak blue bump” (Wills *et al.* 1985) in QSO spectra.

### 3. Discussion

Gravitational lensing could produce the ring morphology observed in MG0248+0641. As an illustration, we have constructed a simple lens model which accounts for the major features in the radio ring (Fig. 9). In this example, an elliptical singular isothermal potential (Blandford & Kochanek 1987) has been placed in front of a background source, which was built up to reproduce the observed structures. Probabilistic calculations based on simple lensing optical depth models (Turner, Ostriker & Gott 1984) suggest that there is 90% confidence for a lens to lie between redshifts 0.07 and 0.27. Assuming a point-mass potential at a redshift of 0.17, which is half the angular diameter distance to a background source at  $772 \text{ h}^{-1} \text{ Mpc}$  ( $\Omega_0 = 1$ ,  $\Lambda_0 = 0$ ,  $H_0 = 70 \text{ km s}^{-1} \text{ Mpc}^{-1}$ ), the observed ring size can be produced by a galaxy with a mass of  $\sim 1 \times 10^{11} M_\odot$  enclosed by the projection of the radio ring. Assuming a factor of five for the ratio of total to enclosed mass, this would imply a galaxy of mass  $\sim 5 \times 10^{11} M_\odot$ . The angular size of the ring corresponds to a line-of-sight velocity dispersion of  $\sim 235 \text{ km s}^{-1}$ , which is typical for galaxies with mass  $\sim 10^{11} M_\odot$ . The modeled lensing galaxy was given an isophotal ellipticity 0.3, and oriented to produce the observed gap at the southern edge of the ring. As shown in Fig. 9, the morphological structure of the western radio lobe can be easily produced with gravitational lensing.

Lens models cannot explain the observed radio polarization, however. Polarization is unaffected

by lensing, so the radial orientation of the polarization vectors along the observed ring would have to correspond to a fortuitous variation along the proposed background jet. Higher resolution radio observations of Einstein ring gravitational lens MG1131+0456 have shown a complex polarization structure (Chen & Hewitt 1993), and such complex polarized intensity distributions are likely to occur in all lenses with ring morphology. The very high fractional polarization values observed are also hard to explain in the context of an ordinary background radio jet. Finally, a very strong objection to the lensing interpretation is the absence of any detectable lensing galaxy, inside the ring radius. An elliptical galaxy with one-dimensional velocity dispersion of  $235 \text{ km s}^{-1}$  would have a luminosity of  $\sim 1 \times 10^{11} L_{\odot}$  (Faber & Jackson 1976), corresponding to an absolute magnitude  $M_R \sim -21$  (Oegerle & Hoessel 1991). The  $k$ -corrected apparent R magnitude is then  $\sim 18.6$ . According to Coleman *et al.* (1980), typical apparent R magnitudes at a redshift of 0.17 are  $\sim 16.2$  for an elliptical, and  $\sim 17.5$  for a spiral galaxy. No source has been found in our optical and infrared data inside the radio ring, where the galaxy is expected, down to a background  $3 \sigma$  surface brightness of  $R \sim 24.8 \text{ mag arcsec}^{-2}$  and  $K \sim 19 \text{ mag arcsec}^{-2}$ . If MG0248+0641 is indeed lensed, then the optical limiting magnitudes suggest an intervening galaxy with mass-to-light ratio at least  $\sim 250$  times higher than that of a typical galaxy (assumed here to have a mass-to-light ratio from 5 to  $15 M_{\odot}/L_{\odot}$ ), which is very large to be associated with a normal galaxy. If the MG0248+0641 ring is indeed caused by gravitational lensing, the implied mass-to-light ratio is estimated to lie in the range 1000–4000, in solar units. At least three candidate “dark” gravitational lenses with similar mass-to-light ratios are known: MG 0023+171 (Hewitt *et al.* 1987), MG 2016+112 (Hattori *et al.* 1997) and Q 2345+007 (Duncan 1991).

The marginally-detected optical source  $3.8''$  west of the radio core is not likely to be the lens. This faint optical source (Fig. 7) lies close to the western hotspot and may well represent optical emission from this hotspot, or from a satellite galaxy of the central quasar, assuming it is at the same redshift as the core. It is also likely that this source is located beyond a redshift of 0.57, given that its R-K color is  $\sim 5.9$ , but exact determination of the photometric redshift is impossible due to the possible presence of dust.

Ring-like morphology in radio sources is also seen in supernova remnants, novae, planetary nebulae, and H II regions, but the radio and optical properties of MG0248+0641 appear to be inconsistent with these interpretations. Given the integrated spectral index, the ring’s angular size, its radio luminosity, and the radial linear polarization vectors, these possibilities are unrealistic; the ring is too large to be an extragalactic supernova, nova, planetary nebula, or H II region, and the non-thermal and steep spectral index distribution of the ring is incompatible with the thermal sources, which have inverted or flat spectral indices. This rules out novae, planetary nebulae, and H II regions. Also, if this ring is due to the interposition of a galactic supernova remnant, the small size of the ring suggests that it is young; between the radio observations of 1980 and 1997, we would have expected to see an expansion in the ring. However, we have not found any evidence for a change in the ring’s physical size. Also, the spectral index of the ring,  $\alpha \sim -1$ , is too steep to be a shell-type supernova remnant, where typically a spectral index of about  $-0.5$  is found. The

location of MG0248+0641, far from the galactic equator at a latitude of  $\sim -45^\circ$ , also suggests a negligible probability that a galactic supernova remnant is superimposed on the radio lobe. We searched the literature for prior radio polarization data on these types of sources, but found none with radial polarization vectors.

The ring-like structure in MG0248+0641 cannot be easily explained within the context of standard radio morphologies. For the observed integrated spectral index of  $\alpha \sim -0.8$ , the maximum degree of linear polarization expected for synchrotron emission is  $\sim 72\%$ , and we see values up to 70% in the circular structure of the western lobe. It is not unusual to see high degrees of fractional linear polarization, exceeding 50%, in the lobes of radio galaxies and quasars, a phenomenon commonly ascribed to shock compression accompanying the transverse expansion of radio lobes and jets (see the 1988 review by Saikia & Salter). Also, very high fractional polarizations, approaching the theoretical maximum, can only be observed if the angle between the plane of compression and the line-of-sight is small. These regions are most likely to be found in the outermost surfaces of the lobes, both where the lobe advances into the intergalactic medium (IGM), and also where the jet hits the hotspot. Terminal hotspots with low polarization suggest high inclination angles for radio galaxies (Laing 1981), i.e. the radio jet axis is pointed close to the line-of-sight. In the case of MG0248+0641, the fractional polarizations in the hotspots are indeed lower than that of the ring-like structure, suggesting that its jets are in fact inclined at a large angle to the plane of the sky. Given this suspected inclination in MG0248+0641, the light propagation delay time between photons from each of the lobes would be expected to cause an asymmetry in the jet lengths; the observed ratio of jet lengths would then suggest that it is the (longer) eastern jet which is approaching. Due to Doppler boosting, this approaching lobe is expected to have a more visible jet, to be brighter, and more polarized; we find instead that these particular features are associated with the (shorter) western jet. Furthermore, if the eastern jet is indeed approaching us, the expected flux ratio between the western and eastern lobes would be less than unity, which is again inconsistent with our observations. Since none of the standard explanations can be used to describe both the flux and length asymmetries in MG0248+0641, we are led to the conclusion that they are intrinsic; the western side of this radio galaxy experiences an environment different from the opposing side.

If the observed ring is due to a disruption of a normal jet to the west of the core, a severe disturbance is required. Unusual structures in extragalactic radio sources have been commonly associated with cD galaxies in cluster centers, where internal dynamics may play a key role. The distribution of X-ray surface brightness in clusters suggests the existence of cooling flows (Fabian *et al.* 1991). Many of these cooling flow clusters have a central dominant galaxy which is associated with a radio source (Burns 1990). However, in our case we find no evidence for a cluster in the field of MG0248+0641. Recent ROSAT observations have not shown any significant X-ray emission, with an upper limit on the observed flux of  $\sim 2 \times 10^{-16} \text{ W m}^{-2}$  (Wolfgang Brinkmann, personal communication). Assuming a temperature of 5 keV, this corresponds to a X-ray luminosity of  $\sim 10^{37} \text{ W}$ , at a redshift of 0.57. The two galaxies we found to the south of the radio core, at a redshift of 0.1, may well belong to a galaxy group, rather than a foreground galaxy cluster.

Other sources with prominent circular lobes and rings have been observed, such as the southern lobe of 3C310 (van Breugel & Fomalont 1984), the northern lobe of 3C219 (Perley *et al.* 1980), and Pictor A (Perley *et al.* 1997), with more such sources listed in van Breugel & Fomalont (1984). At a redshift of 0.57, the projected overall size of MG0248+0641 ( $45 \text{ h}^{-1} \text{ kpc}$ ) and the average diameter of the ring ( $7.5 \text{ h}^{-1} \text{ kpc}$ ) are several times smaller than in these sources. However, the ratio of ring-to-overall size in MG0248+0641 is comparable to many of these sources. The rings in 3C219 and 3C310 are similarly polarized with high fractional values, and electric field intensity vectors oriented in the same configuration as in MG0248+0641. Given that we find no Faraday rotation between 2 and 6 cm, the polarization vectors in Fig. 3 are parallel to the electric field, indicating a circumferential magnetic field. The eastern side of MG0248+0641 is also compatible with the southern side of 3C219, which has been modeled by Clarke *et al.* 1992. These similarities have led us to the tentative conclusion that MG0248+0641 is a small-scale version of sources such as 3C310 and 3C219. However, MG0248+0641 is somewhat different from the known rings in these other sources, which have no terminal hotspots in their lobes (e.g. 3C310). This could likely be due to age differences between the respective lobes, with a smaller, and possibly younger, MG0248+0641 having been energized relatively recently.

The rings in 3C310 and 3C219 are in fact high-intensity spherical shells, with no actual hollow, but rather a decrease in brightness in their central regions. In MG0248+0641, we also find that the minimum brightness at the ring center is slightly higher than the rms noise (off-source), suggesting that the observed ring-like structure is a projected shell-like feature, or a “bubble”. The confinement of such bubbles by a magnetic field and a hot ambient medium can easily produce the observed highly linearly polarized emission. Theoretical predictions of such bubbles, energized by plasma flows, exist in the literature. Smith *et al.* (1983) have predicted such shells of hot gas to be blown out by weak jets, through jet choking and other instabilities in the energy transportation. In 3C310, an optical source has been detected next to the optical counterpart of its core, which has led van Breugel & Fomalont (1984) to conclude that the release of energy in the form of bubbles can be triggered by infalling gas from tidal interaction with this companion. Also, Sadun & Hayes (1993) discovered an optical companion to the core counterpart of Hercules A, with a separation  $\sim 4''$ , and galaxy pairs are found in 3C219 separated by  $\sim 8''$  (Crane, Tyson & Saslaw 1983). Recently, Morrison & Sadun (1996) have argued for a two-stage origin for the multiple rings seen within some extended radio lobes: in the first stage, a periodic outflow and weak shocks form the initial shell structure, with a drift that moves them around, and then the low-pressure portions of these bubbles are filled up with energized electrons in the second stage. The periodic tidal forces from the nearby perturbing companion determine the density modulations, which in turn produce the series of multiple shells.

The production of a shell in the western lobe may also be due to a jet instability. Theoretical predictions suggest that instabilities are likely to occur near the nuclear regions of small and less energetic radio galaxies (Smith *et al.* 1983, and references therein), with more energetic radio galaxies requiring an external source, such as those arising in tidal interactions with other galaxies.



The detection of an optical source  $3''.8$  away from the core counterpart, at the location near the western hotspot of MG0248+0641, is promising within the context of the model of van Breugel & Fomalont (1984). If this is indeed a companion to the central optical source, a tidal interaction may have produced the required instability, allowing a recent outflow of energetic plasma into the western radio jet. The circular structure may also have been due to a past, more active phase of the jet, causing a surge in the gas input to the lobes, and hence a more symmetrical subsequent expansion. Finally, it is also likely that the asymmetry in MG0248+0641 is due to the disruption of the western radio jet as it runs into its companion galaxy.

Since the current models cannot fully describe the energetics required to produce the observed high-intensity shell features, more investigative theoretical work is required in order to describe the above processes, and possibly others not suggested here. The MG0248+0641 field may also be a good candidate for deep observations with the Keck or HST; it would be interesting to search for more direct evidence of galaxy interactions. Also, direct redshift determination of the optical companion may help in accepting or rejecting the interaction hypothesis presented here; however, spectroscopic measurements will be challenging, given its faint magnitude.

We would like to acknowledge Rodney Davies for granting us Director's discretionary time to use MERLIN, Paul Schechter for useful discussions, Rick Perley for pointing out a problem with our initial polarization calibration, and Wolfgang Brinkmann for providing us with results from ROSAT observations of the MG0248+0641 field. The National Radio Astronomy Observatory is a facility of the National Science Foundation operated under cooperative agreement by Associated Universities, Inc. MERLIN is a national facility operated by the University of Manchester on behalf of the Particle Physics and Astronomy Research Council. IRAF is distributed by the National Optical Astronomical Observatories, which are operated by the Association of Universities for Research in Astronomy, Inc., under cooperative agreement with the National Science Foundation. The MDM Observatory is operated by a consortium of the University of Michigan, Dartmouth College and the Massachusetts Institute of Technology. The Multiple Mirror Telescope (MMT) is operated as a joint facility of the Smithsonian Institution and the University of Arizona by the Multiple Mirror Telescope Observatory, and is located on the grounds of the Fred Lawrence Whipple Observatory of the Smithsonian Astrophysical Observatory on Mount Hopkins. This research was supported by NSF grant AST92-24191 at MIT. JL gratefully acknowledges support from NSF grant AST93-03527.

**REFERENCES**

- Becker, R. H., White, R. L., Edwards, A. L. 1991, ApJS, 75, 1.
- Blandford, R., Kochanek, C. 1987, ApJ, 321, 658.
- Browne, I. W. A., Patnaik, A. R., Wilkinson, P. N., Wrobel, J. M. 1997, MNRAS, in press.
- Burns, J. O. 1990, AJ, 99, 14.
- Chen, G. H., Hewitt, J. N. 1993, AJ, 106, 1719.
- Clarke, D. A., Bridle, A. H., Burns, J. O., Perley, R. A., Norman, M. L. 1992, ApJ, 385, 173.
- Coleman, G. D., Wu, C., Weedman, D. W. 1980, ApJS, 43, 393.
- Conner, S. R., Fletcher, A., Herold, L., Burke, B. F. 1993, *Sub-arcsecond Radio Astronomy*, eds. R. J. Davis and R. S. Booth, Great Britain: Cambridge University Press, 154.
- Crane, P., Tyson, J. A., Saslaw, W. C. 1983, ApJ, 265, 681.
- Duncan, R. C. 1991, ApJ, 375, L41.
- Faber, S. M., Jackson, R. E. 1976, ApJ, 204, 668.
- Fabian, A. C., Nulsen, P. E. J., Canizares, C. R. 1991, A&ARv, 2, 191.
- Hattori, M., Ikebe, Y., Asaoka, I., Takeshima, T., Böhringer, H., Mihara, T., Neumann, D.M., Schindler, S., Tsuru, T., Tamura, T. 1997, Nature, 388, 146.
- Herold-Jacobson, L. 1996, MIT Ph.D. Thesis.
- Hewitt, J. N. 1986, MIT Ph.D. Thesis.
- Hewitt, J. N., Turner, E. L., Lawrence, C. R., Schneider, D. P., Gunn, J. E., Bennett, C. L., Burke, B. F., Mahoney, J. H., Langston, G. I., Schmidt, M., Oke, J. B., Hoessel, J. G. 1987, ApJ, 321, 706.
- Hewitt, J. N., Turner, E. L., Schneider, D. P., Burke, B. F., Langston, G. I., Lawrence, C. R. 1988, Nature, 333, 537.
- Hewitt, J. N., Turner, E. L., Lawrence, C. R., Schneider, D. P., Brody, J. P. 1992, AJ, 104, 968.
- Laing, R. A. 1981, ApJ, 248, 87.
- Langston, G. I., Schneider, D. P., Conner, S., Carilli, C. L., Lehár J., Burke, B. F., Turner, E. L., Gunn, J. E., Hewitt, J. N., Schmidt, M. 1989, AJ, 97, 1283.
- Lawrence, C. R., Schneider, D. P., Schmidt, M., Bennett, C. L., Hewitt, J. N., Burke, B. F., Turner, E. L., Gunn, J. E. 1984, Science, 223, 46.

- Lawrence, C. R., Bennett, C. L., Hewitt, J. N., Langston, G. I., Klotz, S. E., Burke, B. F., Turner, K. C. 1986, *ApJS*, 61, 105.
- Lehár J. 1991, MIT Ph.D. Thesis.
- Lehár J., Langston, G. I., Silber, A., Lawrence, C. R., Burke, B. F. 1993, *AJ*, 105, 847.
- Lehár J., Burke, B. F., Conner, S. R., Fletcher, A. B., Irwin, M., McMahon, R. G., Muxlow, T. W. B., Schechter, P. L. 1997, *AJ*, 114, 48.
- Morrison, P., Sadun, A. 1996, *MNRAS*, 278, 265.
- Oegerle, W. R., Hoessel, J. G. 1991, *ApJ*, 375, 15.
- Perley, R. A., Bridle, A. H., Willis, A. G., Fomalont, E. B. 1980, *AJ*, 85, 499.
- Perley, R. A. 1982, *AJ*, 87, 859.
- Perley, R. A., Roser, H. -J., Meisenheimer, K. 1997, *A&A*, in print.
- Sadun, A. C., Hayes, J. J. E. 1993, *PASP*, 105, 379.
- Saikia, D. J., Salter, C. J. 1988, *ARAA*, 26, 93.
- Smith, M. D., Smarr, L., Norman, M. L., Wilson, J. R. 1983, *ApJ*, 264, 432.
- Strom, R. G., Willis, A. G., Wilson, A. S. 1978, *A&A*, 68, 367.
- Strom, R. G., Willis, A. G. 1980, *A&A*, 85, 36.
- Turner, E. L., Ostriker, J. P. Gott, J. R. III 1984, *ApJ*, 284, 1.
- van Breugel, W. L., Fomalont, E. B. 1984, *ApJ*, 282, L55.
- White, R. L., Becker, R. H. 1992, *ApJS*, 80, 211.
- Wills, B. J., Wills, D., Netzer, H. 1985, *ApJ*, 288, 94.

Fig. 1.— VLA A-array 3.6 cm total intensity maps of MG0248+0641. The beam size in the 3.6 cm map is  $0''.3$ , and the peak total intensity is  $22 \text{ mJy beam}^{-1}$ .

Fig. 2.— Spectral index distribution of MG0248+0641, based on VLA 2 and 6 cm observations (grey scale). The contours represent A-array 6 cm total intensity emission, but convolved down to the B-array 2 cm resolution. The ring-like structure has a spectral index of  $\alpha \sim -1.0$ , whereas the unresolved core and hotspot components have flat spectral indices  $\sim -0.5$ .

Fig. 3.— VLA A-array 6 cm total intensity contour maps of MG0248+0641, onto which linear polarization vectors have been overlaid. The natural weighted beam size in the 6 cm map is  $0''.48$ , and is shown in the bottom left corner. In all 3 wavelengths, the fractional polarization vectors are scaled such that  $0''.33$  corresponds to 100%, and they are oriented along the electric field.

Fig. 4.— MERLIN 18 cm total intensity contour map of MG0248+0641, with a restored beam size of  $0''.25$ , which is shown in the bottom right corner. The optical counterpart position from the APM catalog is marked with a cross, scaled to the  $\pm 1''.0$  APM astrometric uncertainty.

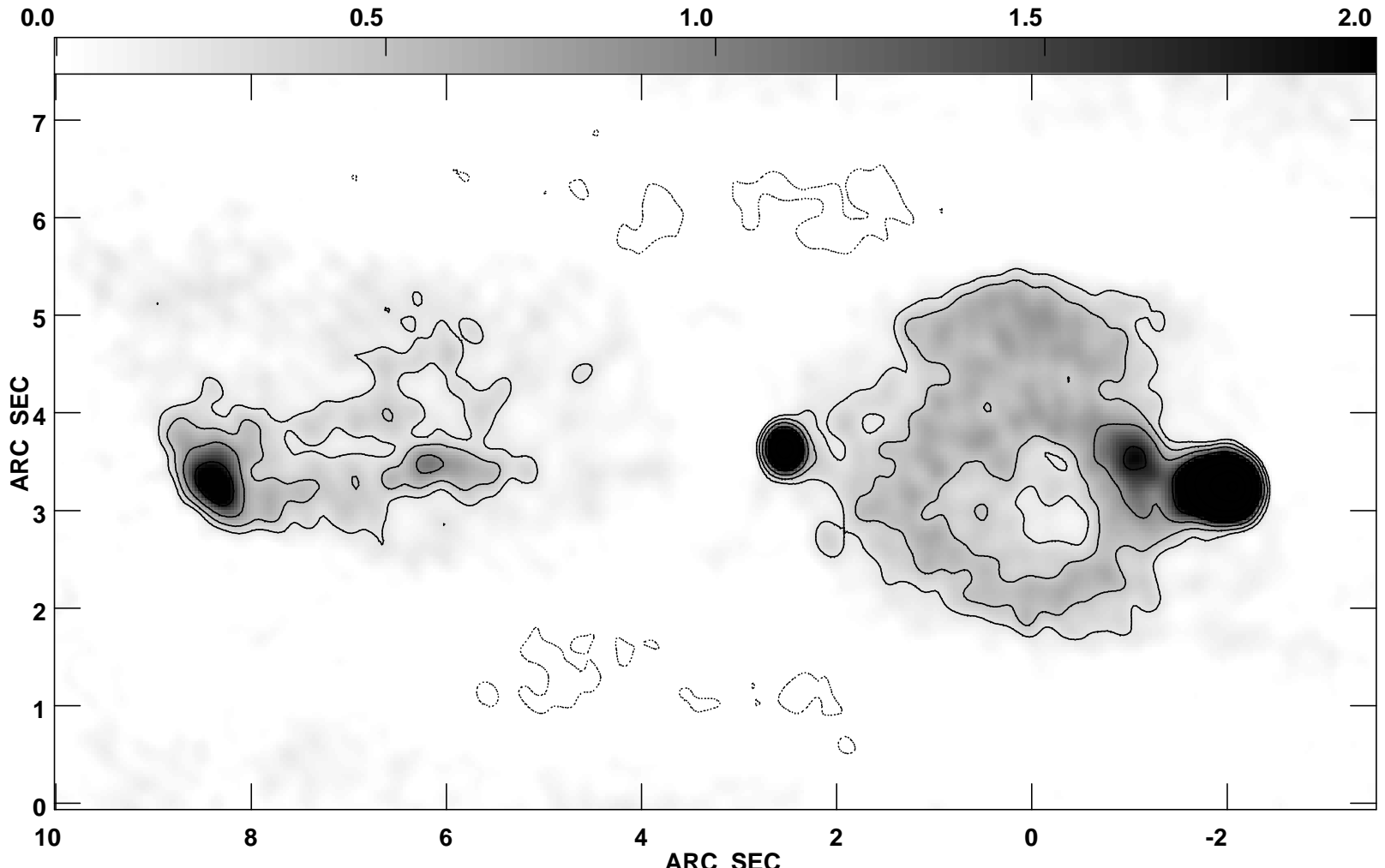
Fig. 5.— MERLIN 18 cm total intensity contour map of MG0248+0641, onto which linear fractional polarization vectors have been overlaid. The vectors are scaled such that one arcsecond of vector length corresponds to 50%, and they are oriented along the electric field.

Fig. 6.— R band optical CCD image, with a total integration time 3000 seconds, of the MG0248+0641 field ( $4.5'$  by  $4.5'$ ), observed with the MDM 2.4 m telescope. North is left; east is down. The counterpart is marked with a square box. The limiting magnitude is  $\sim 25$ . The pixel scale is  $0''.275$ .

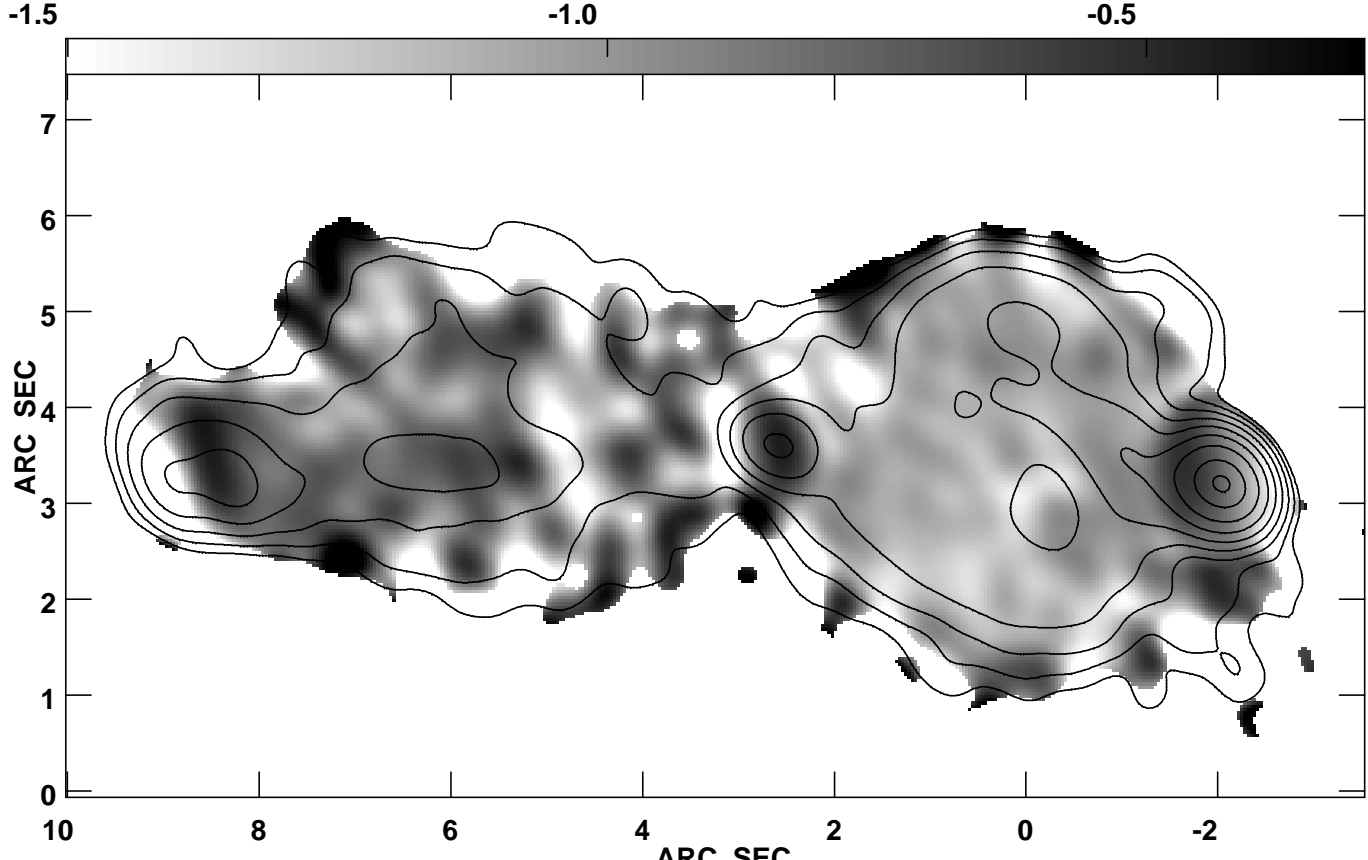
Fig. 7.— MDM 2.4 m R band image overlaid on the 3.6 cm VLA map, with contours in steps of the  $2 \sigma$  noise level in the optical data. We have positioned the optical core counterpart such that it lies on top of the radio core. A faint optical source is marginally detected close to the western hotspot, at a level of  $2.1 \sigma$ .

Fig. 8.— The optical spectrum of the counterpart of core component (A), taken at the MMT with the Blue Channel Spectrograph. Wavelength is in angstroms, and the flux is normalized. The spectrum shows the “weak blue bump”, and Mg II and [O III] emission lines, from which we calculate a redshift of 0.57. The prominent absorption near  $7600 \text{ \AA}$  is a sky feature.

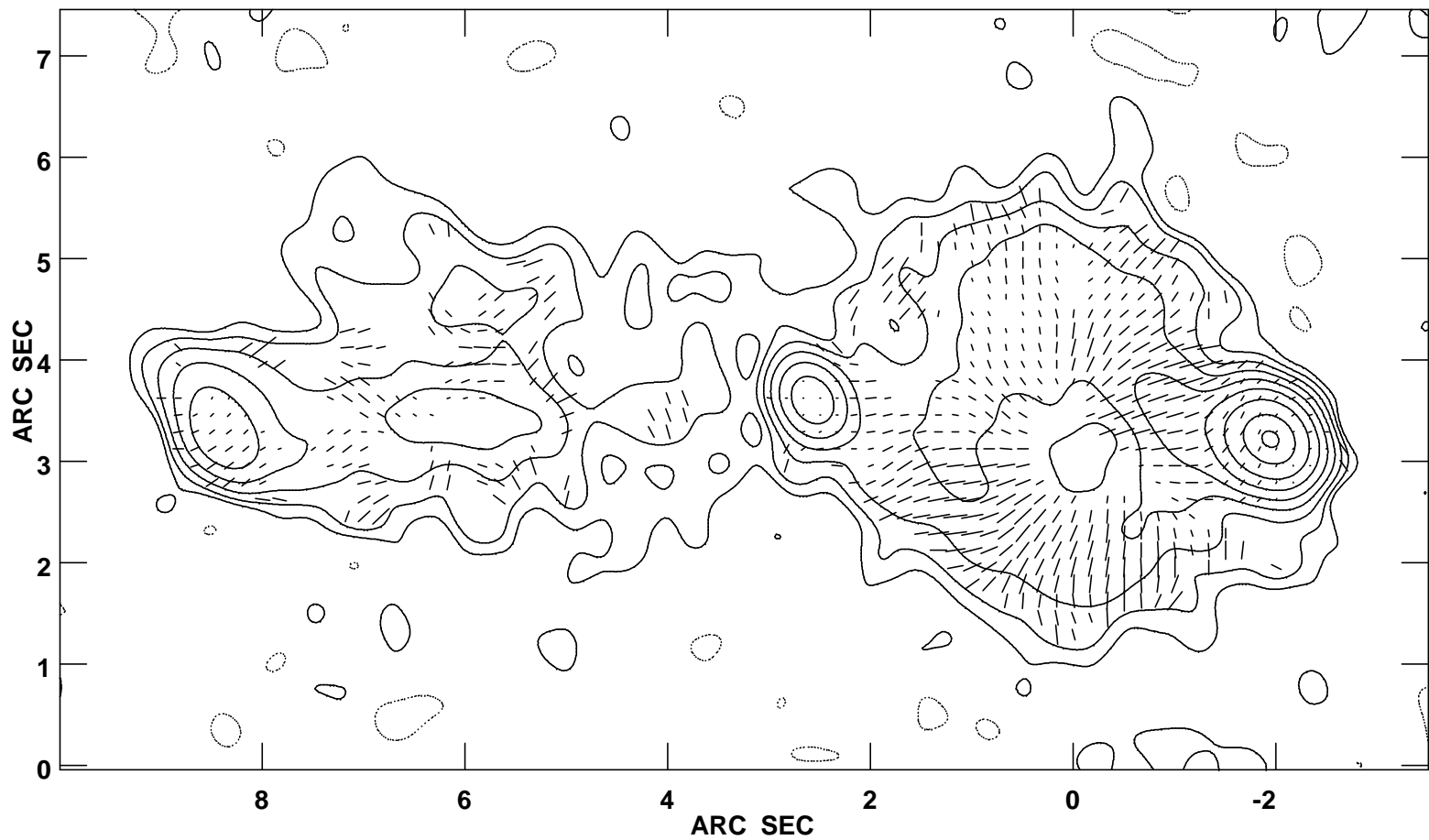
Fig. 9.— Lens model interpretation for MG0248+0641. The contours in the source plane show the background source as it would appear without lensing, and the diamond caustic is drawn in bold. The image plane shows the same source projected through the lens model, with the tangential critical line drawn in bold. The source was constructed to roughly produce the observed structures.



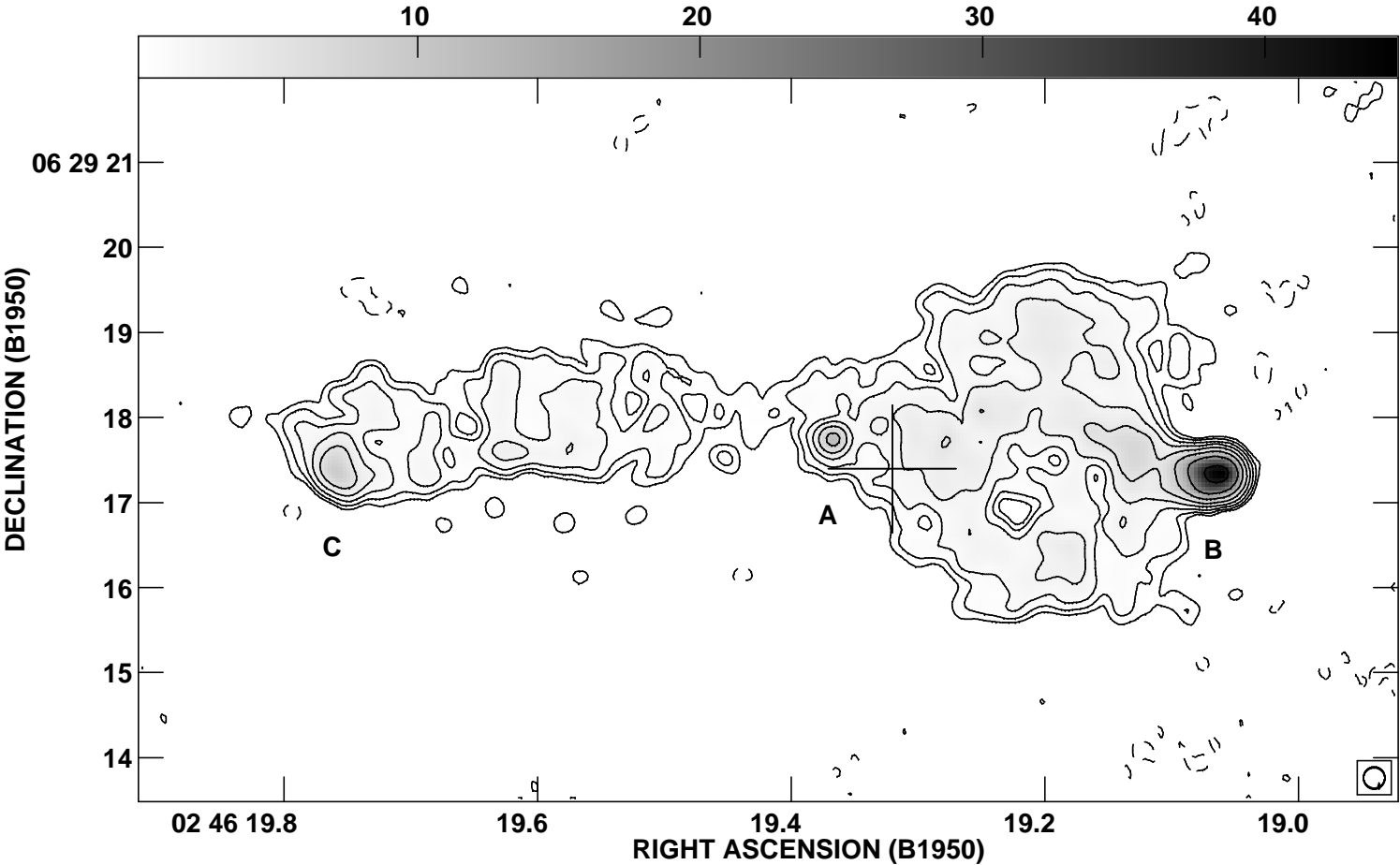
Center at RA 02 48 58.10000 DEC 06 41 40.0000  
Grey scale flux range= 0.000 2.000 Millijy/BEAM  
Peak contour flux = 2.1973E-02 JY/BEAM  
Levs = 2.1973E-04 \* ( -1.00, 1.000, 2.000,  
4.000, 8.000, 16.00, 32.00, 64.00, 95.00)



Center at RA 02 48 58.1000 DEC 06 41 40.000  
Grey scale flux range= -1.500 -0.300 SP INDEX  
Peak contour flux = 6.0145E-02 JY/BEAM  
Levs = 6.0145E-04 \* ( -0.500, 0.500, 1.000,  
2.000, 4.000, 8.000, 16.00, 32.00, 64.00,  
95.00)

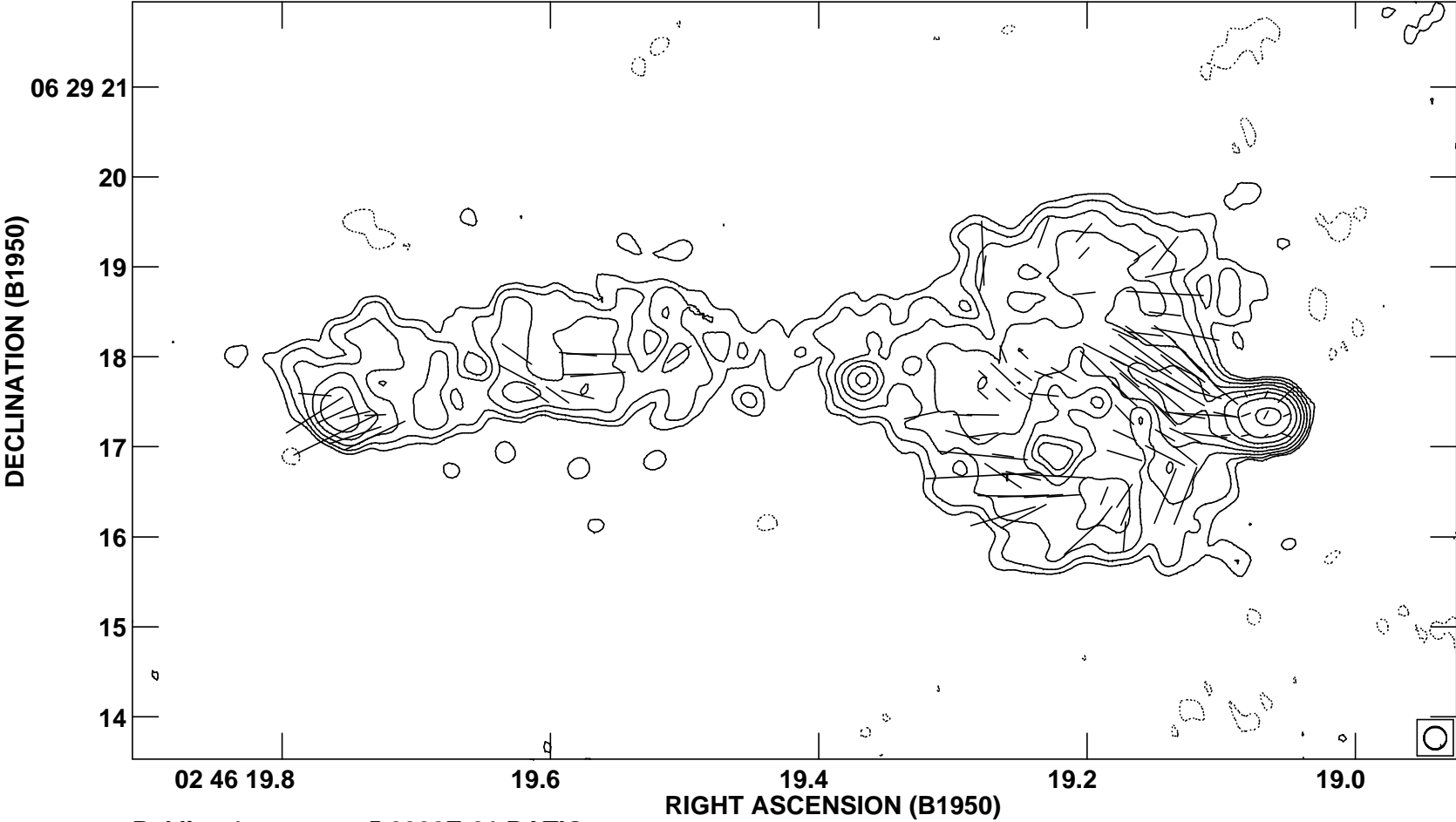


Center at RA 02 48 58.1000 DEC 06 41 40.0000  
Pol line 1 arcsec = 3.0000E+00 RATIO  
Peak flux = 2.5814E-02 JY/BEAM  
Levs = 2.5814E-04 \* ( -0.500, 0.500, 1.000,  
2.000, 4.000, 8.000, 16.00, 32.00, 64.00,  
95.00)

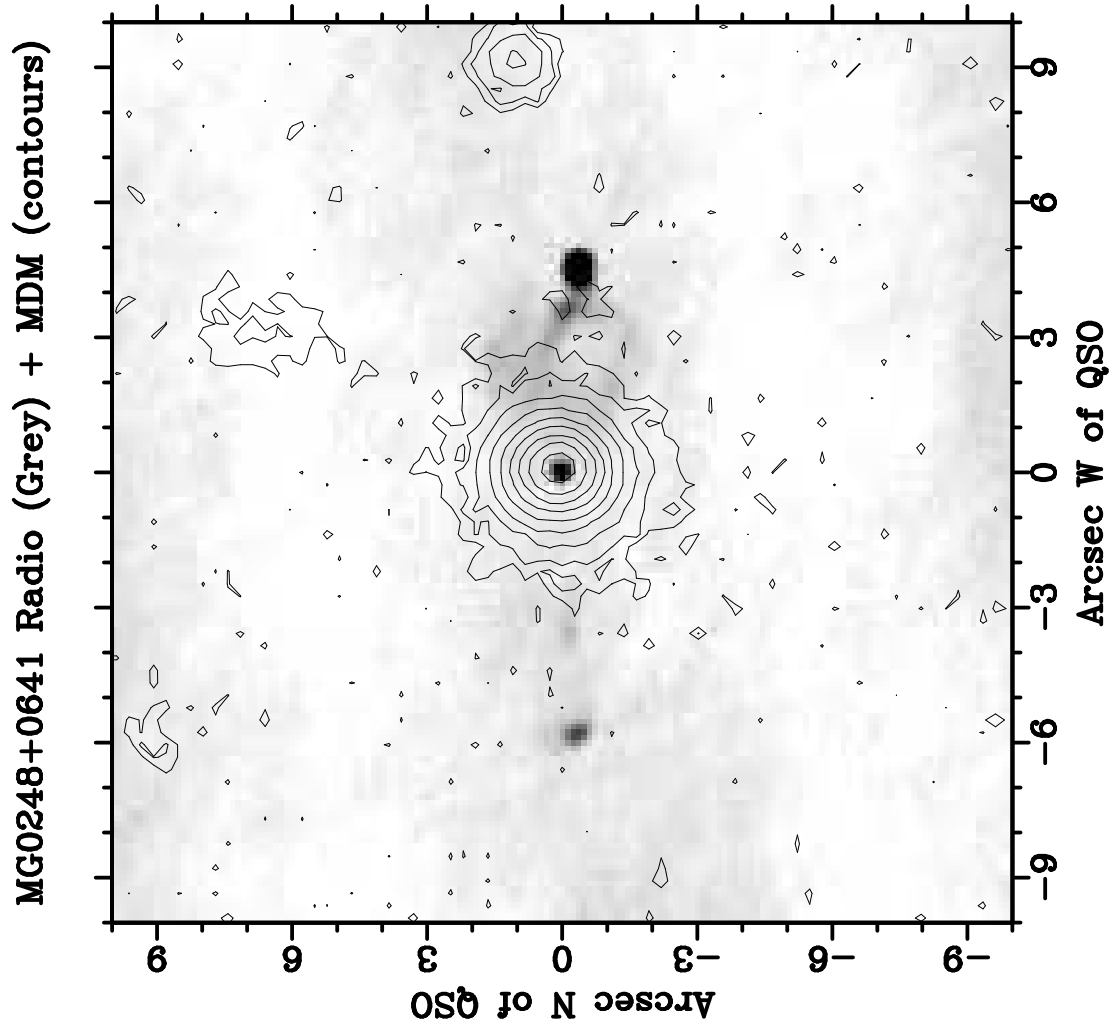


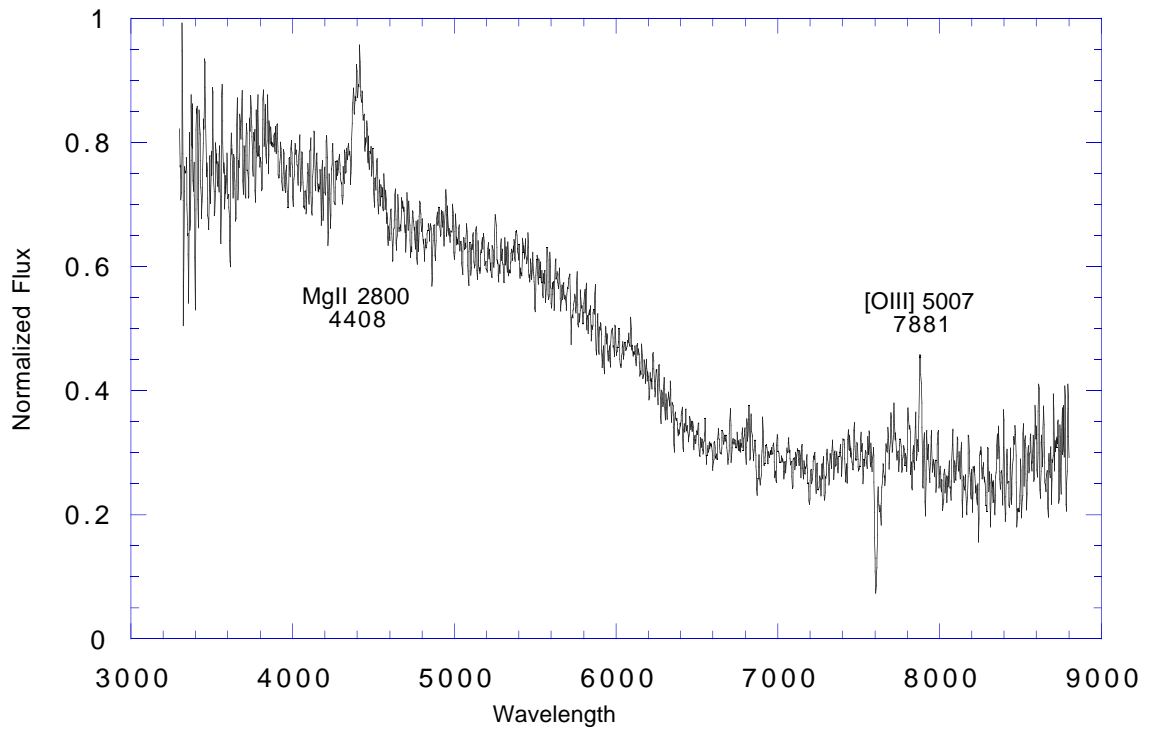
Grey scale flux range= 0.3 44.6 MilliJY/BEAM  
Cont peak flux = 4.4579E-02 JY/BEAM  
Levs = 3.0000E-04 \* ( -1.00, 1.000, 2.000,  
4.000, 8.000, 16.00, 32.00, 64.00, 128.0,  
256.0, 512.0, 1024.)

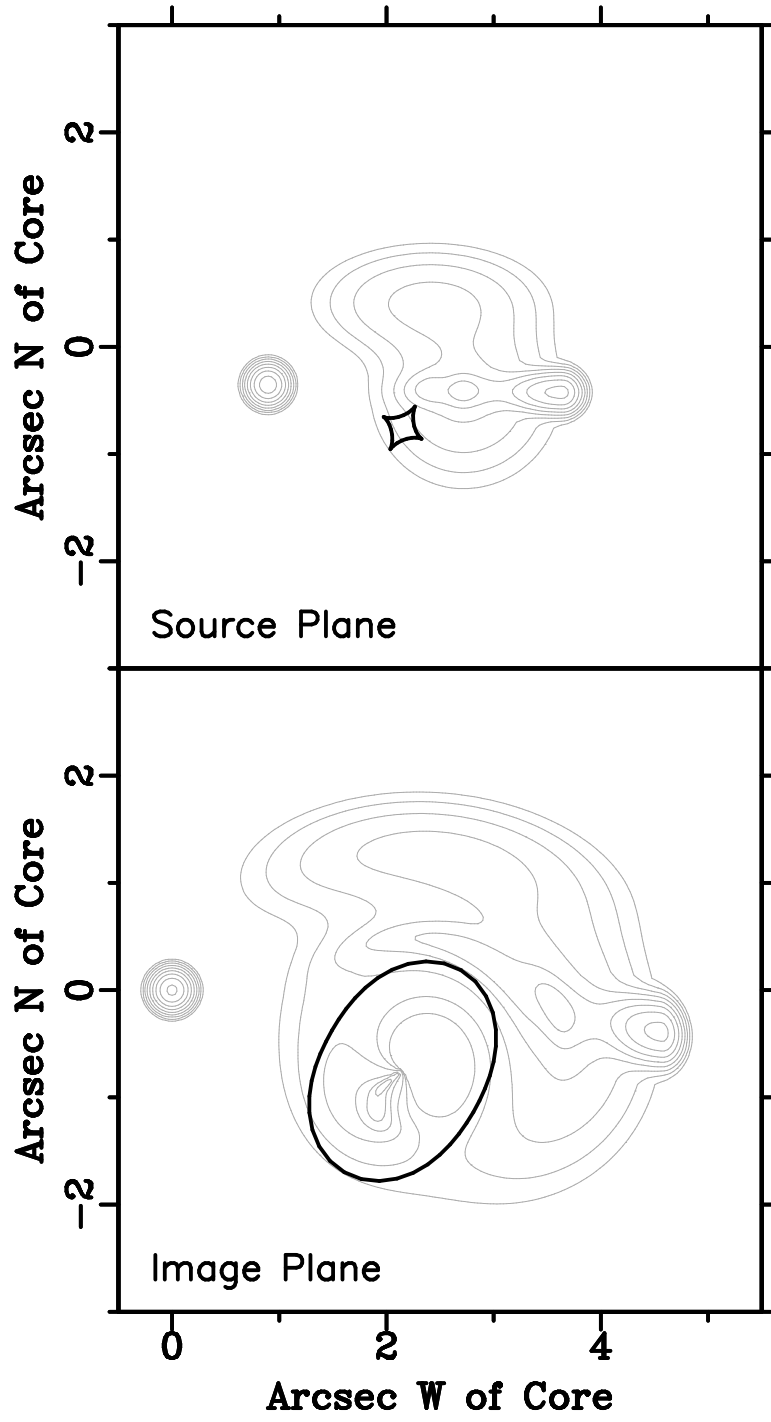




Pol line 1 arcsec = 5.0000E-01 RATIO  
Peak flux = 4.4579E-02 JY/BEAM  
Levs = 3.0000E-04 \* ( -1.00, 1.000, 2.000,  
4.000, 8.000, 16.00, 32.00, 64.00, 128.0,  
256.0, 512.0, 1024.)







This figure "fig6.gif" is available in "gif" format from:

<http://arxiv.org/ps/astro-ph/9708152v3>